



# Influence of Granular Columns on the Behavior of Reinforced-Soil Wall on Layered Soft Foundation

Amir Hossein Mirrashed<sup>1</sup> · Iman Hosseinpour<sup>1</sup> · Seyed Hamed Mirmoradi<sup>2</sup> · Hadi Ahmadi<sup>3</sup>

Accepted: 20 March 2022 / Published online: 31 March 2022

© The Author(s), under exclusive licence to Springer Science+Business Media, LLC, part of Springer Nature 2022

## Abstract

This paper numerically investigates the effectiveness of granular columns on the performance of a reinforced soil wall (RSW) along the construction period. The column wall methodology was employed to convert the granular columns into the plane strain configuration. Following model validation with field data, the influence of critical factors including soft soil and granular column strength properties as well as basal reinforcement is examined in terms of foundation deformations, wall facing deflection, tension in geogrid reinforcements, and wall short-time stability. The results showed that columns' diameter and their center-to-center spacing had the significant impact on RSW performance among others, as the magnitude of wall deformations and facing deflection were found to be significantly influenced by the granular columns. The internal friction angle of column materials, however, was shown to have a negligible influence on wall performance. In addition, using a high stiffness reinforcement at the base of the wall remarkably improved its deformations over soft foundation, thus enhancing its stability during working stress conditions.

**Keywords** Geosynthetics · Reinforced soil wall · Soft soil · Granular columns · Finite element analysis

## 1 Introduction

Reinforced soil walls (RSWs), since their first employment in the 1980s, have been frequently used through the globe in geotechnical engineering projects (Rowe and Ho, 1993). These types of retaining structures have many advantages over conventional walls (e.g., gravity walls, rigid concrete, or cantilever walls) such as low cost, rapid construction, flexibility, and good performance under seismic loading (Ehrlich

---

✉ Iman Hosseinpour  
imanhp@guilan.ac.ir

Extended author information available on the last page of the article

and Mirmoradi, 2013; Chenari et al., 2020; Srikar and Mittal, 2020; Bathurst and Naftchali, 2021). Moreover, RSWs can tolerate large differential settlement and show acceptable stability compared to traditional walls; thus, they are highly adaptable and can be constructed on unsuitable lands (Rowe and Skinner, 2001; Chen et al., 2014; Damians et al., 2014).

However, when RSWs are constructed over soft or very soft clayey foundations, they undergo excessive total deformations which may cause wall instability during construction; thus, foundation treatment using either rigid piles or granular columns is unavoidable (Han, 2015; Hosseinpour et al., 2014, 2017; Bahadori et al., 2018; Lima et al., 2019; Zheng et al., 2019; Ghorbani et al., 2021; Aghili et al., 2021). Among other deep improvement techniques, compacted granular columns hold several advantages such as reducing differential settlements, increasing bearing capacity, and accelerating consolidation process by the provision of radial drainage (Han and Ye, 2001; Ambily and Gandhi, 2007; Hosseinpour et al., 2015, 2021, 2022; Sexton et al., 2016; Almeida et al., 2018; Alkhorshid et al., 2021). Despite numerous studies on the effect of RSW geometrical properties and toe conditions on the performance of the wall, the influence of foundation treatment, particularly application of granular columns, has been rarely investigated.

Mirmoradi et al. (2021) studied the influence of foundation conditions in combination with other factors such as wall height, reinforcement stiffness, and facing type on the behavior of reinforced soil walls under working stress conditions. This study showed that the foundation soil may affect the wall behavior as low foundation stiffness increased the maximum tensile force developed in the reinforcement layers located close to the wall base.

Ezzein and Bathurst (2008) studied the influence of foundation compressibility on the response of reinforced soil walls. Physical modeling was carried out on two 1/6-scale reinforced soil wall tests to isolate the influence of vertical foundation compressibility on wall behavior. Results of experiments showed that foundation compressibility significantly altered the mobilized tensions in the reinforcement layers and affected the wall stability.

Ehrlich and Mirmoradi (2013) and Mirmoradi and Ehrlich (2016) reported that a combination of toe fixities and facing stiffness controls the wall behavior, rather than each factor in isolation. Later Mirmoradi and Ehrlich (2017) included wall height as another critical factor to be considered in the abovementioned combination. They concluded that for a vertical wall, the influence of toe resistance and facing stiffness on the variations of maximum mobilized tension is limited to 4 m above the wall base. Similarly, Palmeria and Monte (1997) and Schmertmann et al. (1989) demonstrated that a yielding foundation may increase the lateral deflection of the wall facing and the tension mobilized in the reinforcement layers placed near the base of the wall.

It is eminent from all the above studies that the combined effect of wall geometry, toe restriction, and foundation compressibility on the behavior of the RSWs was fairly well recognized. However, there are no studies available on the influence of foundation treatment on the short-time performance of the RSW when it is assumed to be constructed over a soft clay layer strengthened with granular columns. In the current study, therefore, the behavior of a RSW constructed over a soft foundation

improved by a group of granular columns is numerically investigated. Following model validation with measured data, the wall performance is analyzed in terms of wall deformations at the base, facing deflection, and mobilized tensions in reinforcement layers as well as variations of excess pore water pressure in the clayey foundation during rapid construction.

## 2 Model Description and Validation Analysis

Data provided from a full-scale reinforced soil wall (Chen et al., 2014) was used to perform the numerical analyses. As schematically illustrated in Fig. 1a, fourteen layers of uniaxial geogrid were used to reinforce the backfill soil of a 7.6-m-high wrapped-facing wall. The geogrid reinforcements were 10 m in length placed at an equal vertical spacing of 0.5 m. The geogrid had an axial stiffness of 620 kN/m calculated at 5% strain and also an ultimate strength of 70 kN/m. As illustrated in Fig. 1b, the wall was constructed over 190 days with consolidation intervals between loading stages allowing the excess pore water pressure to gradually dissipate. Stage construction of the wall was simulated by activating the fill materials in several phases in accordance to the actual time of fill placement and consolidation intervals as illustrated in Fig. 1b. The soil stratigraphy underneath the wall mainly consisted of layered compressible clayey soil with a total depth of 31 m from the ground surface with their geotechnical properties given in Table 1.

Before the wall construction, a 1.6-m-thick preliminary fill and a 0.6-m-thick sand cushion were placed under the wall base to facilitate the construction activities. These layers also prevented further settlements of the wall during the construction stages due to their high stiffness compared to the compressible foundation. In addition, 12-m-long prefabricated vertical drains (PVDs) with center-to-center spacing of 1.5 m were installed in a triangular pattern to hasten the consolidation process during rapid construction.

In the current study, numerical simulation was carried out using two-dimensional finite element code *PLAXIS-2D 8.6* (Brinkgreve and Vermeer, 2002). The finite element model used to perform the numerical analysis is shown in Fig. 2. It is noted that the finite element model adopted for validation analysis, material properties, and constitutive models are all exactly similar to those presented in Chen et al. (2014). The model geometry and soil stratigraphy are the same as the real condition described above. Regarding the model boundary conditions, roller fixities were assigned to the lateral borders to prevent any horizontal movement along the vertical sides while the model was fully fixed along the base. The groundwater table level was also set to the interface between the preliminary fill and the top of soft clay layer, as observed in situ. Concerning the material constitutive models, the linear elastic-perfectly plastic Mohr–Coulomb (MC) failure criterion was adopted to simulate the behavior of preliminary fill, sand cushion, and backfill soil materials. However, the hardening soil model (HS), i.e., a hyperbolic soil model, was assigned for all clay layers.

The geogrid reinforcement was modeled as an isotropic linear geogrid element available in *PLAXIS*, which could sustain only tensile force along its length. A

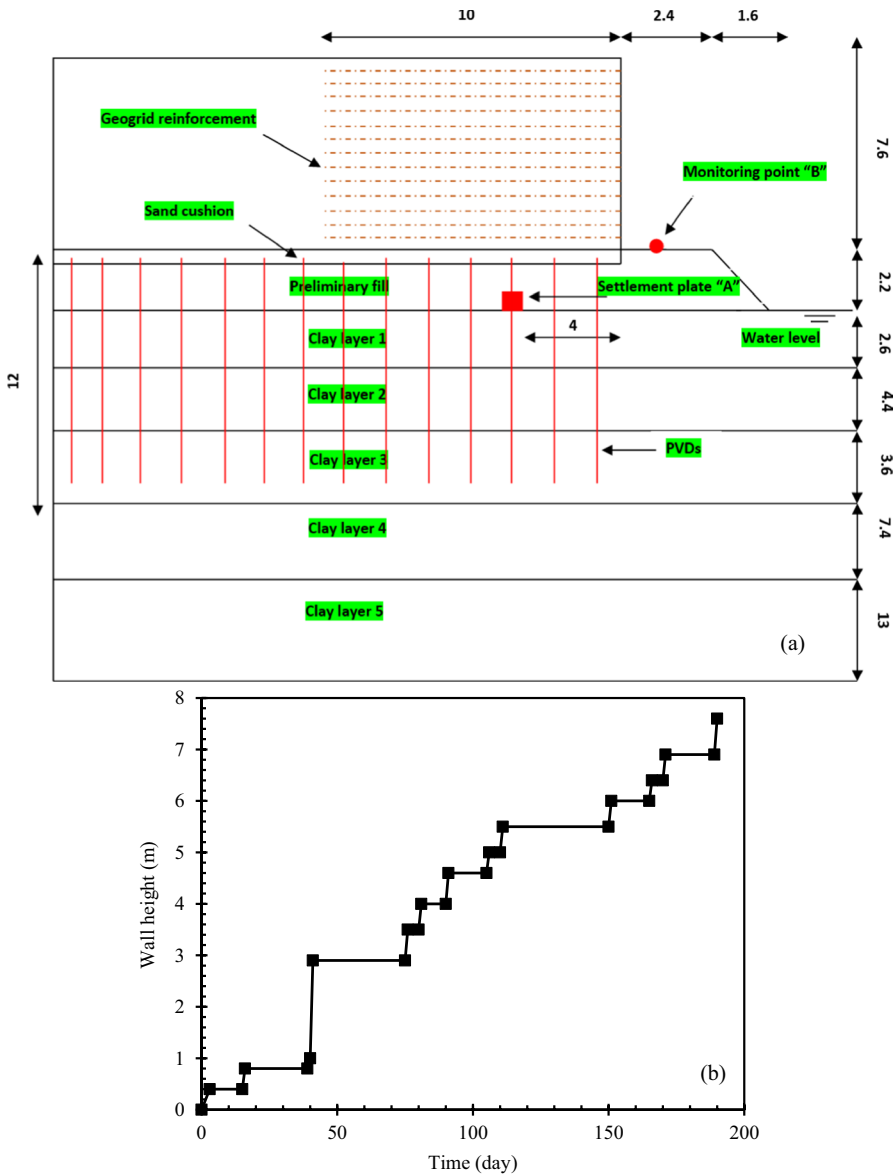


**Fig. 1** Details of the wall construction over PVDs improved soft foundation adopted from Chen et al., (2014): **a** wall geometry and subsoil profile (dimensions are in meter); **b** construction stages over time

perfect bonding was assigned along the interface between the geogrid element and the surrounding soil. Previous studies have shown that using the perfect interface adherence under working stress conditions results in a reasonable prediction

**Table 1** Geotechnical properties of different soil layers (Chen et al., 2014)

Properties	Backfill and preliminary fill	Sand cushion	Clay layer 1	Clay layer 2	Clay layer 3	Clay layer 4	Clay layer 5
Constitutive model	MC	MC	HS	HS	HS	HS	HS
Material type	Drained	Drained	UU	UU	UU	UU	UU
$\gamma_{unsat}$ (kN/m <sup>3</sup> )	19	17	13.6	12.8	12.1	15.4	15.1
$\gamma_{sat}$ (kN/m <sup>3</sup> )	19	20	18.4	17.9	17.5	19.5	19.3
$k_{hp}$ (m/day)	—	4.32	3.18E-05	3.26E-05	2.76E-05	1.38E-04	1.38E-04
$k_{hv}$ (m/day)	—	4.32	9.85E-05	9.33E-05	1.15E-04	1.04E-05	1.04E-05
$E_{ref}$ (MPa)	5	20	—	—	—	—	—
$E_{ref}^{50}$ (MPa)	—	—	3.18	2.12	2.47	8.37	5.7
$E_{oed}^{ref}$ (MPa)	—	—	3.18	2.12	2.47	8.37	5.7
$E_{ur}^{ref}$ (MPa)	—	—	9.54	6.36	7.41	25.1	17.1
$m$ (-)	—	—	1	1	1	1	1
$\nu$ (-)	0.33	0.2	0.25	0.25	0.25	0.2	0.2
$c'$ (kPa)	16	1	7	7	6	17	18
$\phi'$ (°)	30	30	27.9	28	24.9	29.8	31.2

$\gamma_{unsat}$  unsaturated unit weight;  $\gamma_{sat}$  saturated unit weight;  $k_{hp}$ , equivalent horizontal permeability in plane strain condition;  $k_{hv}$ , equivalent vertical permeability in plane strain condition;  $E_{ref}^{50}$ , secant elastic modulus at confining pressure of 100 kPa;  $E_{oed}^{ref}$ , oedometric elastic modulus;  $E_{ur}^{ref}$ , elastic modulus of soil for unloading and reloading;  $m$ , power for stress-level dependency of stiffness;  $\nu$ , Poisson’s ratio;  $c'$ , drained cohesion;  $\phi'$ , drained internal friction angle; *UU*, unconsolidated undrained; *MC*, Mohr–Coulomb; *HS*, hardening soil

of the measured data (e.g., Hatami and Bathurst, 2005; Tandel et al., 2012; Mirmoradi and Ehrlich, 2016).

The PVDs were simply defined using drain elements available in *PLAXIS* which are vertical lines inside the geometry of the model. In a consolidation analysis, the excess pore pressures are set to zero in all nodes belong to the drain. In other words, vertical drain elements have infinite permeability coefficient value thus providing radial drainage along its length during the consolidation analysis.

Preliminary mesh sensitivity analysis was also performed to verify the influence of mesh coarseness on the predicted results. As seen in Fig. 3, the difference between the maximum deformations computed using very fine and fine mesh was less than 5%; thus, no further mesh refinement was needed. Therefore, a fine mesh was utilized to divide soil clusters into triangular elements as it resulted in a reasonable estimation of the behavior of the studied RSW.

The results of finite element analysis are compared to measured data in Fig. 3 where the ground settlement at point A and the vertical and horizontal displacements at wall toe at point B are plotted against time. Figure 3a shows that the adopted numerical model could adequately predict the variation of the ground settlement at point “A” vs. time. Both numerical analysis and measured data exhibit approximately 65-cm ground settlement at the end of 190th day.

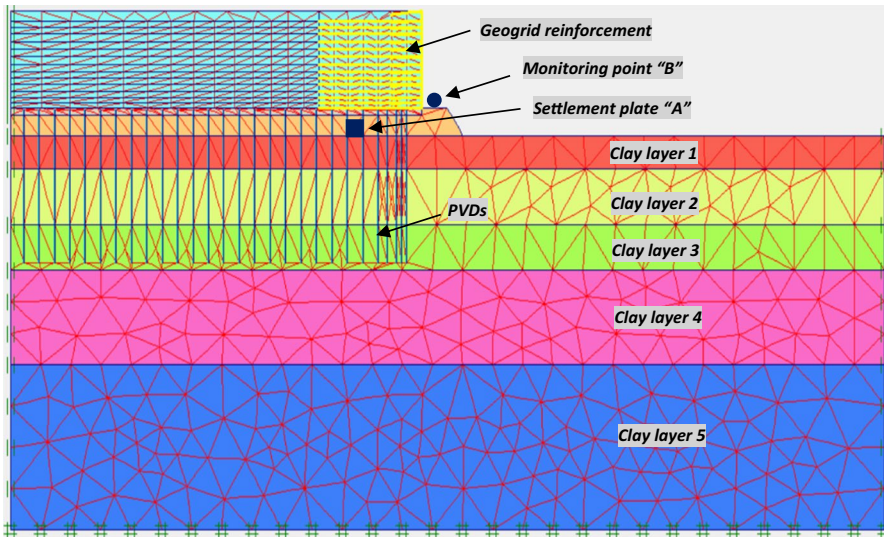


**Fig. 2** Finite element model used to perform the numerical analysis

Figure 3b displays variations of the measured and calculated vertical displacements at wall toe (i.e., point B) versus time. It can be observed that there is a good agreement between maximum values as well as some extent of measured and computed trends. However, there is a slight difference between the two curves along the day of 50 to 100, which could be attributed to the discrepancy between the actual and simulated loading stages.

Figure 3c compares measured and calculated horizontal displacements at wall toe (i.e., point B). It can be seen that the numerical results could predict fairly well the measured values at any stage of wall construction as well as consolidation intervals. According to the validation analysis, it is observed that the present numerical model could suitably represent the actual behavior of the studied RSW and thus can be further used to perform the parametric analyses.

### 3 Column Wall Methodology

To investigate the influence of granular columns, the PVDs penetrated underneath the studied RSW are all removed and substituted by a group of granular columns which are simulated herein using column wall methodology proposed by Zhang et al. (2014). The method is ideally an effective solution for the conversion of a complicated three-dimensional problem of a column-supported embankment into a two-dimensional plane strain configuration. In this contribution, the granular column is modeled as a continuous shear wall for which the strength properties of aggregate materials are accordingly recalculated to

account for the geometrical and mechanical properties of the granular column and surrounding soft soil.

Herein, the hypothetical granular columns are assumed to be 10.6 m long passing through the clay layers 1, 2, and 3. The strength and mechanical properties of the granular column materials are suitably selected to be within the values recommended in the literature (Briaud, 2013; Almeida et al., 2018) as listed in Table 2. In the column wall methodology, the geometrical properties of the granular columns, i.e., diameter and spacing, are similar to those of the actual condition while the equivalent properties are required to be calculated considering the strength properties of the granular columns and the surrounding soft soil using equations below (Zhang et al., 2014):

$$E_w = E_c a_r + E_s (1 - a_r) \quad (1)$$

$$c_w = c_s (1 - a_r) \quad (2)$$

$$\phi_w = \tan^{-1} (a_r \tan \phi_c + (1 - a_r) \tan \phi_s) \quad (3)$$

where  $E_w$ ,  $c_w$ , and  $\phi_w$  indicate to the elastic modulus, cohesion, and friction angle of equivalent column wall, respectively. The parameters  $E_c$  and  $E_s$  are the elastic modulus of a single granular column and soft soil, respectively. In addition, the parameter  $c_s$  is the soft soil cohesion, and  $\phi_s$  and  $\phi_c$  correspond to the drained friction angle of the soft soil and aggregate materials, respectively. Moreover,  $a_r$  is the area replacement ratio which is calculated using (Almeida et al., 2018):

$$a_r = \frac{A_c}{A_E} \quad (4)$$

where  $A_c$  and  $A_E$  indicate the cross-sectional area of granular column and unit cell (i.e., influence area), respectively. The latter is, however, calculated based on the columns' installation pattern and their spacing. In the course of this study, for the columns installed in a square grid, the parameter  $A_E$  is equal to  $1.13S$  where  $S$  is columns' center-to-center spacing.

## 4 Parametric Analyses

A set of comprehensive parametric analyses was carried out to investigate the effect of granular columns on the overall behavior of the RSW described above. Firstly, the column wall methodology was adopted to simulate the granular columns in plane strain condition and then the effect of granular columns and host soft soil properties was analyzed. It is noted that, in the plane strain idealization, the granular columns were simulated with the width equal to their diameter while the equivalent mechanical properties were calculated to account for the effect of columns diameter (i.e., area replacement ratio) using Eqs. 1 to

**Fig. 3** Comparison between measured data and numerical analysis: **a** ground settlement at point A; **b** settlement at point B; **c** horizontal displacement at point B

3. Table 3 represents the magnitude of variables considered in the parametric analyses.

#### 4.1 Influence of Column Diameter

Figure 4 shows the variations of the total deformations calculated under the wall toe (i.e., point B) for different values of the granular columns' diameter. In these analyses, the center-to-center spacing between the columns was kept constant equal to  $S=2$  m while the columns' diameter varies between the values mentioned in Table 3. Accordingly, granular columns installed in a square pattern with different diameters of 30, 60, 90, and 120 cm yield to the area replacement ratio equal to 1.8%, 7%, 16%, and 29%, respectively.

As shown in Fig. 4a, an increase in the columns' diameter significantly reduces the magnitude of the toe settlement at the end of wall construction (i.e., day of 190). In addition, increasing columns' diameter causes the settlement development to follow a gentle slope meaning that time to settlement stabilization reduces by increasing columns' diameter.

Profile of the soil horizontal deformation below the wall toe (i.e., point B) up to 10 m underneath the ground surface is illustrated in Fig. 4b for various columns' diameters. It is observed that increasing columns' size greatly diminishes the maximum value of the soil horizontal deformation, and subsequently improves the stability of the wall against deep-seated failure caused by excessive lateral movement. For instance, an increase in columns' diameter from 30 to 120 cm leads to four times reduction in the maximum soil horizontal deformation which in turn improves wall stability during construction.

This behavior can be seen in Fig. 5a where the variation of the excess pore water pressure vs. time in the middle of the clay layer 1 is plotted for different columns' diameter. According to the numerical results, the diameter of the granular columns (i.e., area replacement ratio) plays a significant role in development and dissipation of excess pore water pressure. It is seen that increasing columns' diameter from 0.3 m to 1.2 m decreases the maximal excess pore pressure from 34 to 12 kPa indicating that the larger column size considerably accelerates the consolidation process.

This observation can be interpreted by two main functions of compacted granular columns: first, the larger granular columns reduce the amount of the total stress transferred to the soft soil; thus, the maximal excess pore pressure decreases (Almeida et al., 2018; Hosseinpour et al., 2019). Secondly, increasing column size improves the rate of radial drainage; thus, time to pore pressure dissipation significantly decreases (Barron, 1948).

Stability analysis was also conducted using Phi-C reduction method which is an option available in *PLAXIS* to calculate the factor of safety at the end of wall construction. In the Phi-C reduction approach, the soil strength properties (i.e.,



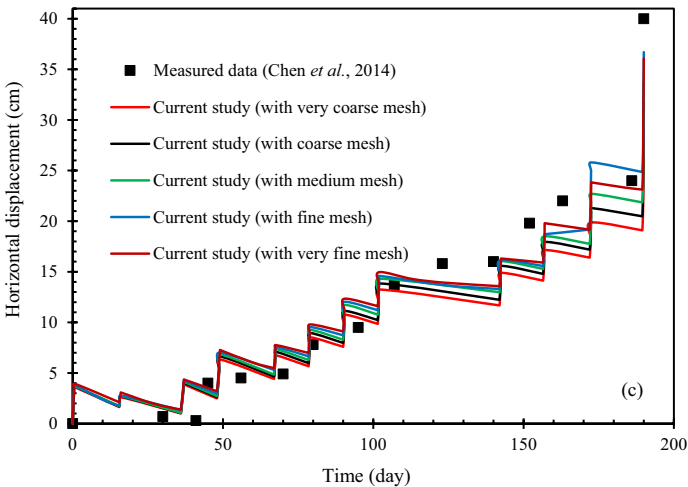
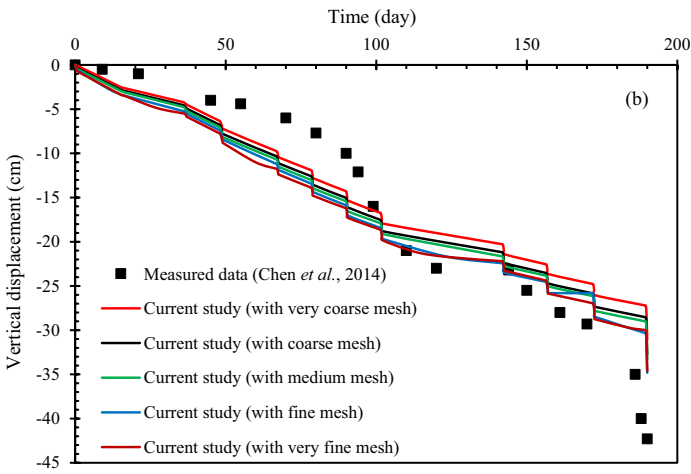
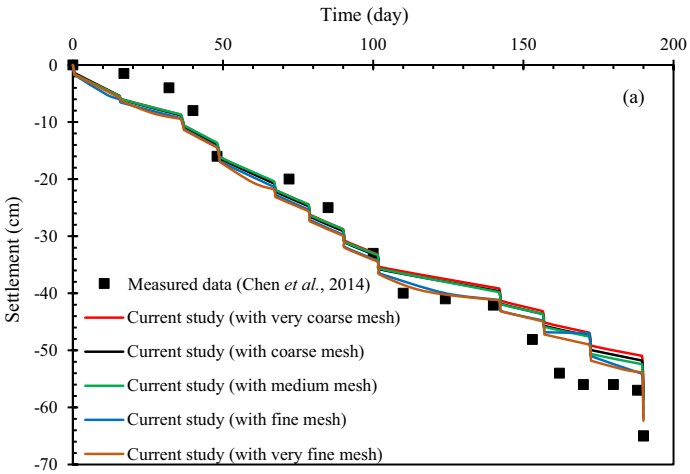


**Table 2** Properties of the granular column materials used in numerical analyses

Properties	Column diameter, $d_c$ (cm)	Unit weight, $\gamma_c$ (kN/m <sup>3</sup> )	Elastic modulus, $E_c$ (MPa)	Poisson's ratio, $\nu$ (-)	Cohesion, $c$ (kPa)	Friction angle, $\phi_c$ (°)
Value	50	20	40	0.3	0	38

$\tan \phi$  and  $c$ ) are gradually decreased until failure of structure occurs. Following the factor of safety is calculated by the ratio of available strength to strength at failure. As seen, a larger column diameter improves the undrained stability of RSW along with the rapid construction which is reflected in Fig. 5b. For instance, enlarging column diameter from 0.3 m to 1.2 m increases FS value from 1.09 (i.e., almost failure) to 1.23. The influence of the granular column size on the shear failure mechanism is vividly observed in Fig. 6 where the shear failure surface is compared for two column diameters. It is seen that the larger column diameter prevents the failure surface to cross the underneath weak soil; thus, the deep-seated failure surface turns into the local shear failure.

The influence of granular columns' diameter on the performance of the studied RSW is evaluated in terms of the wall facing deflection and maximum tensile force in the geogrid reinforcements as illustrated in Fig. 7. Based on the numerical results, increasing columns' diameter remarkably reduces the wall facing deflection and thus enhancing its performance during construction. As seen in Fig. 7a, the magnitude of facing deflection reduces from 82 cm to about 30 cm as granular columns' diameter increases from 0.3 m to 1.2 m. The maximum mobilized tension in geogrid layers is displayed in Fig. 7b as granular columns' diameter changes. The figure shows that the distribution of the maximum reinforcement loads with wall height is better represented by a triangular shape which is in agreement with the results reported by Mirmoradi and Ehrlich (2015, 2016). The illustrated trend also shows that as the columns' diameter increases, the maximum mobilized tensile force tends to decrease. However, this behavior is much more pronounced when the columns' diameter of 1.2 m was employed in the analysis.

## 4.2 Influence of Columns' Spacing

Figure 8 represents the total deformation under the wall toe for various values of spacing between the columns. In this analysis, the columns were 50 cm in diameter while their spacing varied between the values listed in Table 3. It should be noted that, to compare the effect of columns' spacing and diameter, the columns' spacing was changed within the range to reproduce the area replacement ratio values of 1.8%, 7%, 16%, and 29%, equal to those when columns' diameter changed. As shown in Fig. 8a, a closer installed granular column significantly reduces the magnitude of settlement at the end of wall construction. For instance, by reducing the column spacing from 3.33 m to 1.11 m, the final settlement would decrease almost 43%. Moreover, the settlement-time curve displays a gentle trend meaning that less

**Table 3** Variables considered in the parametric analysis

Parameter	Value
Granular columns' diameter, $d_c$ (cm)	30, 60, 90, 120
Columns center-to-center spacing, $S$ (m)	0.83, 1.11, 1.67, 3.33
Soft soil cohesion, $c_s$ (kPa)	7, 15, 30, 45
Friction angle of column aggregates, $\phi_c$ ( $^\circ$ )	30, 35, 40, 45
Basal reinforcement stiffness, $J$ (kN/m)	500, 1000, 2000, 4000, 6000

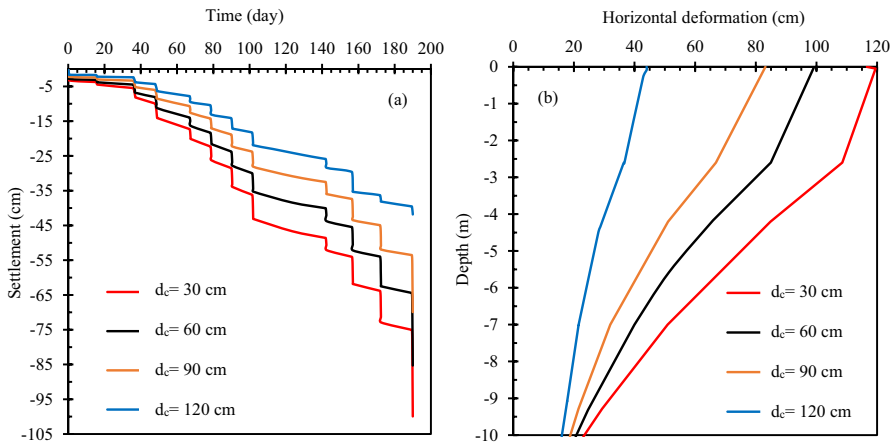


**Fig. 4** Influence of column diameter on total deformations of the wall ( $S = 2$  m): **a** settlement vs. time; **b** profile of soil horizontal deformation ( $S = 2$  m,  $c_s = 15$  kPa,  $\phi_c = 38^\circ$ ,  $J = 1000$  kN/m)

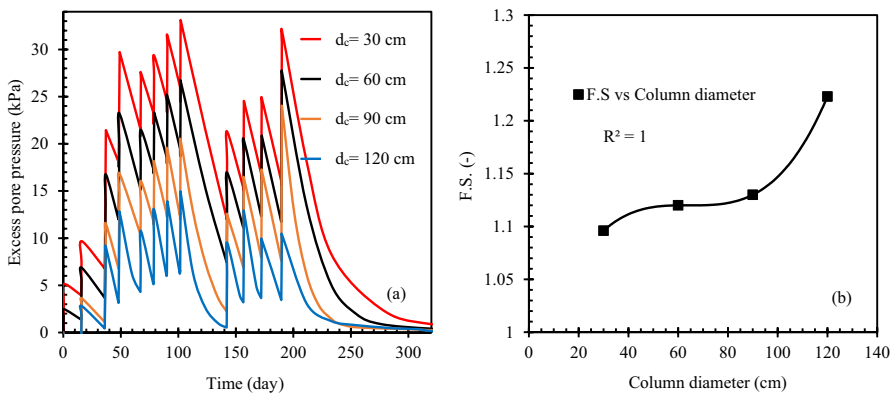


**Fig. 5** Influence of granular column diameter on: **a** variation of excess pore pressure in the middle of clay; **b** factor of safety at the end of construction

time for settlement stabilization is required as columns' center-to-center spacing decreases.

Profile of the subsoil horizontal deformation under the wall toe for different spacing values is also shown in Fig. 8b. It can be seen that, as the columns are placed at a closer distance, subsoil horizontal displacement is greatly diminished. For example, reducing columns' spacing from 3.33 m to 1.66 m decreases the magnitude of maximum horizontal displacement to half (i.e., from 185 to 91 cm), subsequently improving wall stability during rapid construction against failure due to excessive foundation horizontal movement (Abusharar and Han, 2011).

The positive effect of columns' spacing on excess pore pressure in the middle of clay layer 1 is evident in Fig. 9a. It can be observed that decreasing columns' spacing significantly reduces the maximum value of excess pore pressure. For example, reducing columns' spacing from 3.33 m to 1.66 m shatters the maximum excess pore pressure from 47.2 kPa to 25 kPa. The reason behind

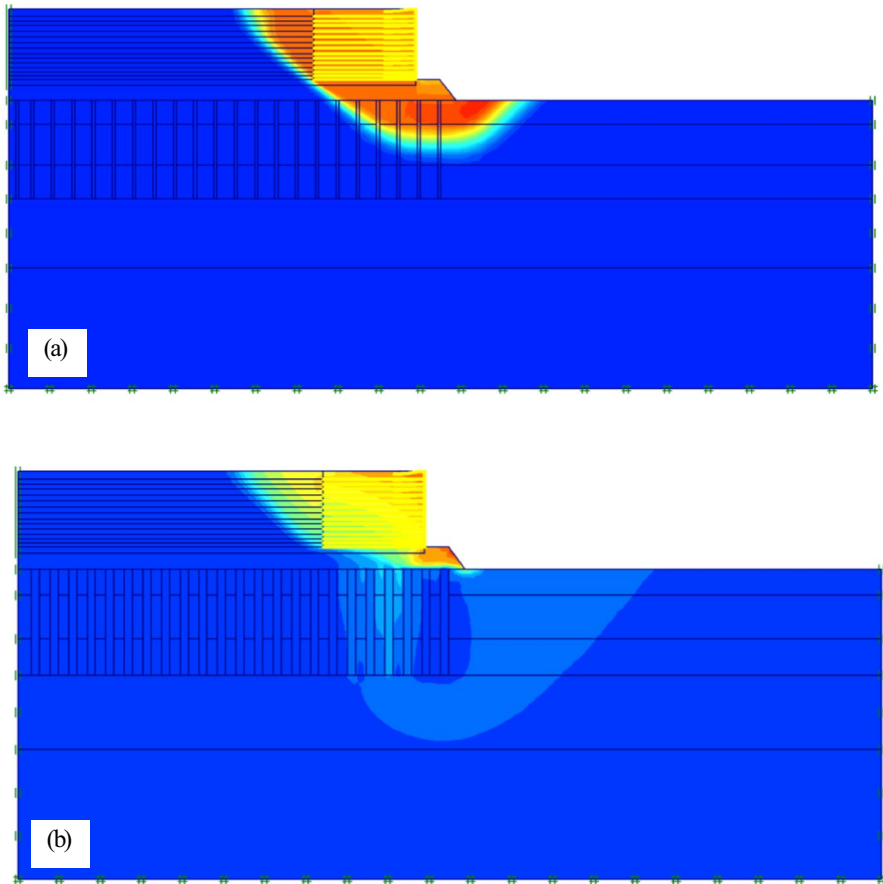


**Fig. 6** Computed failure surface for different column diameters: **a**  $d_c = 30$  cm; **b**  $d_c = 120$  cm

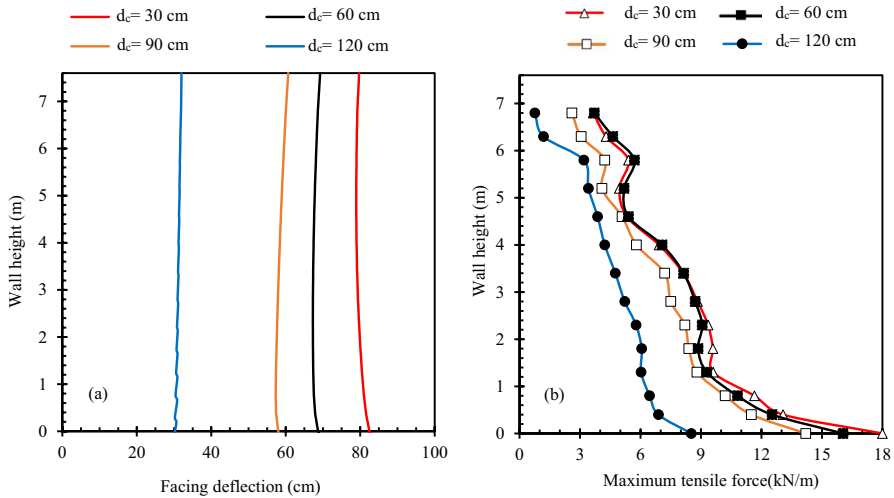


**Fig. 7** Influence of granular column diameter on the performance of the wall: **a** facing deflection; **b** geogrid maximum tensile force

this observation is attributed to the change in the distribution of the total vertical stress under RSW as columns’ spacing varies. In fact, the granular columns installed in a closed grid attract a larger portion of the total vertical stress; thus, the total stress transferred to the soft soil and subsequent excess pore pressure would be significantly reduced.

In addition, a closer distance between the granular columns facilitates consolidation by providing a shorter flow path, hence hastening the excess pore pressure dissipation and time to settlement stabilization, as well. This behavior can be indirectly interpreted by Fig. 9b where variations of safety factors are plotted as columns’ spacing changes. It is observed that reducing columns’ spacing improves RSW short-time stability. In other words, granular columns installed in a closer grid lead to a faster gain in strength (or improved degree of consolidation) of saturated soft clay which in turn helps the bearing capacity of the foundation soil to enhance during rapid construction (Almeida and Marques, 2013). A direct comparison between Figs. 5b and 9b reveals that using larger columns to keep the same area ratio seems to result to a more considerable factor of safety rather than reducing columns’ spacing. As observed in Fig. 9b, using 80-cm-diameter granular columns spaced at  $S = 1.11$  m ( $a_r = 7\%$ ) results to a FS value of about 1.14. However, 120-cm-diameter columns spaced at  $S = 2$  m to reproduce the same  $a_r$  value yields to a FS = 1.25 (see Fig. 5b) confirming the more pronounced role of granular columns’ size on FS value compared with columns’ spacing.

The influence of columns’ spacing is also analyzed in terms of RSW facing deflection and maximum mobilized tension in geogrid reinforcements. As shown in Fig. 10a, the center-to-center spacing between granular columns greatly affects the magnitude of facing deflection. It can be seen that reducing columns’ spacing from 3.33 m to 1.66 m decreases facing deflection by about 100%. Nevertheless,

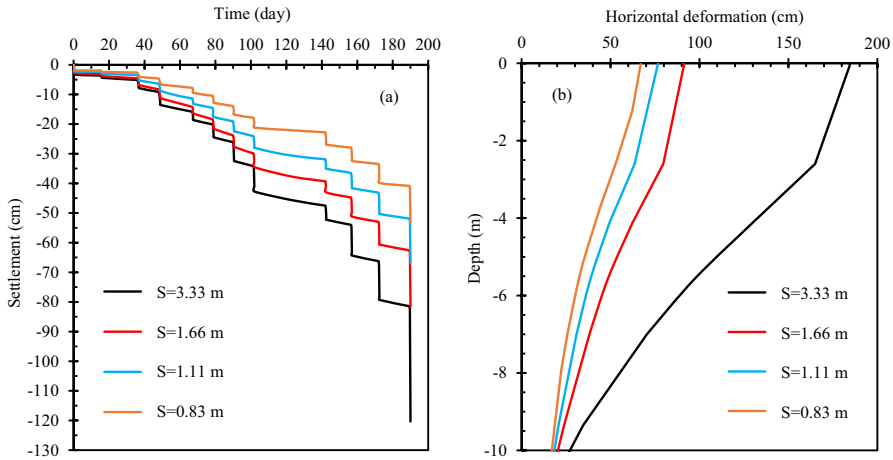


**Fig. 8** Influence of column spacing on total deformations at wall toe: **a** settlement vs. time; **b** profile of soil horizontal deformation ( $d_c = 50$  cm,  $c_s = 15$  kPa,  $\phi_c = 38^\circ$ ,  $J = 1000$  kN/m)

when columns' spacing decreases from 1.66 m to 0.83 m, no further significant reduction is seen as facing deflection decreases only 18%.

Figure 10b displays the maximum tensile force mobilized in each geogrid layer for different values of columns' spacing. As observed the maximum reinforcement load is not significantly influenced by the columns' spacing up to 1.66 m. When the spacing of 3.33 was employed in the analysis, however, the maximum reinforcement loads increased in the reinforcement layers placed near the foundation (almost 3 m above the base of the wall). This is in accordance with the results presented by Mirmoradi and Ehrlich (2017) and Mirmoradi et al., (2021), who investigated the

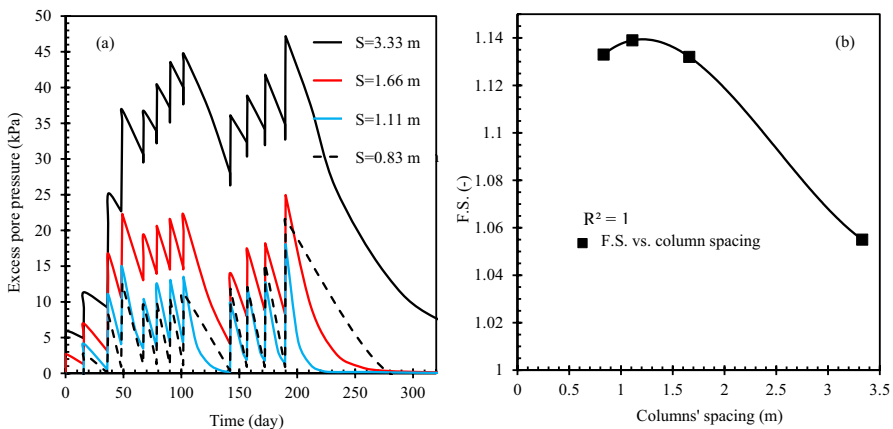


**Fig. 9** Influence of columns' spacing on: **a** excess pore pressure in the middle of clay; **b** factor of safety at the end of construction

importance of foundation stiffness and toe resistance on the performance of reinforced soil structures.

### 4.3 Influence of Soft Soil Cohesion

As expressed in Eq. (2), the equivalent column wall cohesion  $c_w$  is linearly dependent on the magnitude of soft soil cohesion  $c_s$ . Therefore, the influence of the equivalent cohesion  $c_w$  on the performance of the studied RSW is assessed herein by a change in the soft soil undrained cohesion  $c_s$  within the values presented in Table 3. In these analyses, the granular columns are 80 cm in diameter with a center-to-center spacing of 2 m.

As shown in Fig. 11a, an increase in soft soil cohesion  $c_s$  greatly affects the trend and the magnitude of settlement at the end of wall construction. As seen, increasing undrained cohesion from 7 to 15 kPa reduces approximately 43% of settlement at wall toe. Further reduction can be also observed when  $c_s$  value increases up to 40 kPa, but not as significant as when  $c_s$  improves from 7 to 15 kPa which reflects the significant effectiveness of the application of granular columns in soft deposits. In addition, the settlement vs. time curve exhibits a smoother trend as soft soil cohesion increases indicating lowered post-construction settlement as soft soil cohesion improves. Profile of the subsoil horizontal displacement illustrated in Fig. 11b also indicates that assigning a higher  $c_s$  value to the soft soil layer minimizes soil lateral displacement underneath the wall toe. Similar to settlement, this improvement is much more significant when  $c_s$  value increases from 7 to 15 kPa as the maximum horizontal displacement reduces to half confirming the efficiency of granular columns in controlling the horizontal deformations of RSW over compressible foundation.

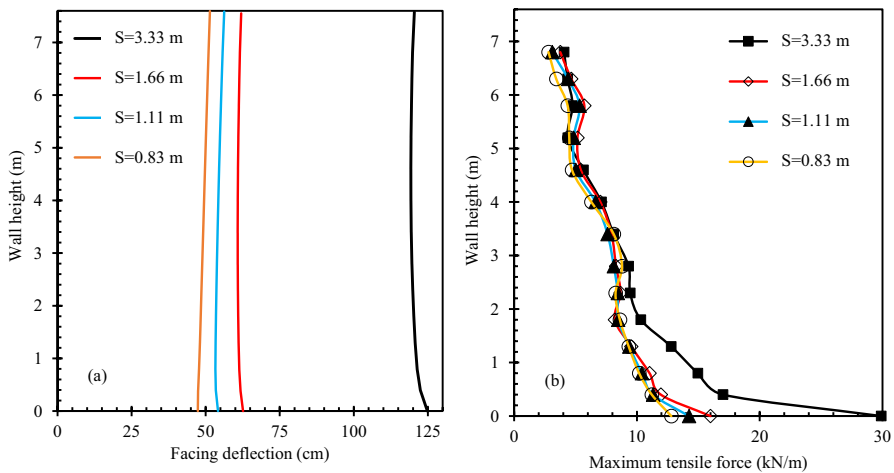


**Fig. 10** Influence of columns' spacing on the performance of the wall: **a** facing deflection; **b** geogrid maximum tensile force

Variation of the excess pore water pressure in the middle of clay layer 1 illustrated in Fig. 12a shows that increasing soft soil cohesion reduces maximum excess pore pressure during construction. As seen, increasing  $c_s$  value from 7 to 30 kPa causes the peak value of excess pore pressure reduces from 26 kPa to around 12 kPa. However, the dissipation time remains almost untouched and does not display any noticeable improvement. Indeed, the soft clay having a greater  $c_s$  value attracts a higher portion of the wall applied stress in quasi-undrained condition, thus resulting a lower part of the total stress to be converted into the excess pore water pressure. The satisfactory effect of soft soil cohesion on RSW stability improvement is also shown in Fig. 12b. The linear trend of the factor of safety improvement with soft soil cohesion indicates the most significant effectiveness of soft soil undrained strength on improvement of the wall short time performance, among others.

The effect of soft soil cohesion on RSW performance is further extended by evaluating facing deflection and geogrid maximum tension as displayed in Fig. 13. Facing deflection profile at the end of construction for various values of soft soil cohesion is shown in Fig. 13a. As seen, increasing soft soil cohesion greatly reduces extensive facing deflection and improves wall performance over soft clay layer. The magnitude of facing deflection reduces to almost half (i.e., from 62.5 cm to about 32 cm) as soft soil cohesion increases from 7 to 15 kPa. The maximum tensile force for all reinforcement layers at the end of RSW construction is plotted in Fig. 13b. As soft soil cohesion increases, tensile force in geogrid layers tends to decrease since a more firm stratum underneath results in a lowered strain in reinforcement layers. Based on the numerical results, increasing  $c_s$  value from 7 to 15 kPa has shown to reduce the tensile force by about 43%, particularly, for lower reinforcement layers. However, the influence of  $c_s$  improvement on either wall-facing deflection or reinforcement tension seems to be less significant for  $c_s$  values higher than 30 kPa.

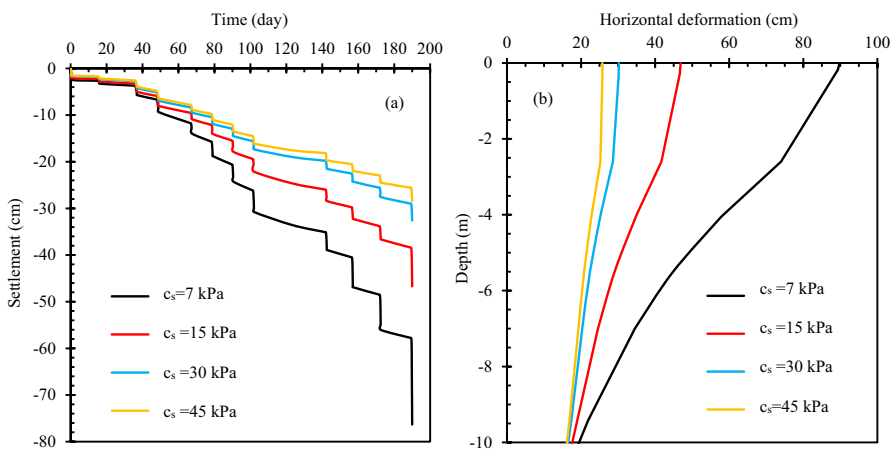


**Fig. 11** Influence of soft soil cohesion on total deformations of the wall: **a** settlement vs. time; **b** profile of horizontal soil deformation ( $S=2$  m,  $d_c=80$  cm,  $\phi_c=38^\circ$ ,  $J=1000$  kN/m)



### 4.4 Influence of Friction Angle of Column Materials

Figure 14a displays the time-settlement curve calculated at the wall toe for different values of friction angle of granular column materials. In these analyses, the granular columns are 80 cm in diameter and installed in a center-to-center spacing equal to 2 m. Using Eq. (3), an increase of friction angle from 30 to 45 degrees for an individual column does not yield a significant increase in equivalent column wall friction angle, and thus settlement vs. time curves will remain approximately unchanged. Profile of the subsoil lateral displacements for different values of column diameter exhibits similar behavior as shown in Fig. 14b indicating the negligible influence of friction angle of column materials on soil horizontal deformation beneath the RSW.

The negligible effect of friction angle of column materials on magnitude and variations of excess pore pressure is reflected in Fig. 15a. As can be seen, neither peak excess pore pressure and dissipation time is not remarkably influenced by change in friction angle of column materials as all curves are approximately coincident. Results of numerical analysis also indicate the insignificant influence of internal friction angle of column materials on wall stability as the values of safety factor do not remarkably change when friction angle increases from 30° to 45°.

Moreover, wall-facing deflection and maximum mobilized tensile force computed at the end of construction are compared when column friction angle changes. As illustrated in Fig. 16a, wall-facing deflection is not remarkably affected as column friction angle is increased. The insignificant influence of increasing friction angle is again observed in maximum mobilized tensile force confirming that friction angle of column materials may have the least impact on the behavior of RSW over soft foundation (Ghorbani et al., 2021; Tandel et al., 2012).

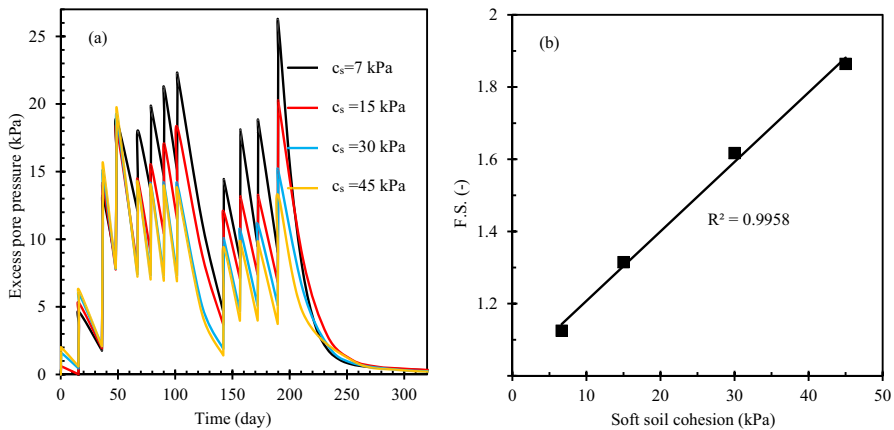


**Fig. 12** Influence of soft soil cohesion on **a** excess pore pressure in the middle of clay; **b** factor of safety at the end of construction

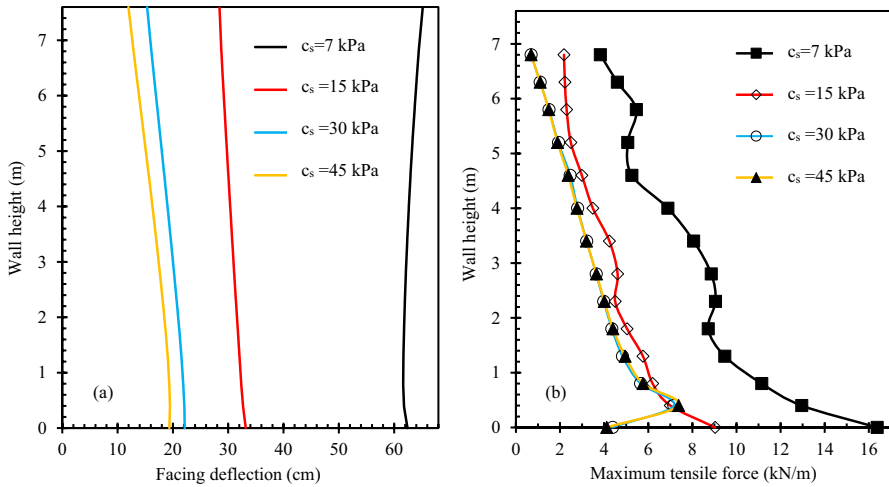


**Fig. 13** Influence of soft soil cohesion on the performance of the wall: **a** facing deflection; **b** geogrid maximum tensile force

### 4.5 Influence of Basal Reinforcement

Using basal reinforcement for stability improvement and load transfer mechanism under the reinforced embankments is well researched in literature (Girout et al., 2014; Yoo, 2015; Fagundes et al., 2017). The foundation and fill soils induce strains on the geosynthetic as they displace horizontally. The geosynthetic reacts and a resistant tensile force is mobilized, restricting displacement of the compressible soil layer. To investigate the effect of basal reinforcement stiffness on the behavior of the studied RSW, a geogrid layer is placed along the wall base. The granular columns’

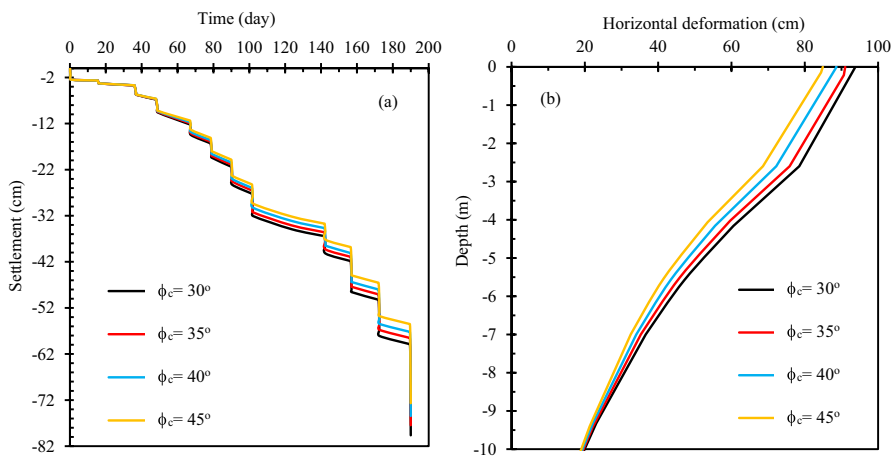


**Fig. 14** Influence of friction angle of column materials on total deformations of the wall: **a** settlement vs. time; **b** profile of soil horizontal deformation ( $S = 2$  m,  $d_c = 80$  cm,  $c_s = 15$  kPa,  $J = 1000$  kN/m)

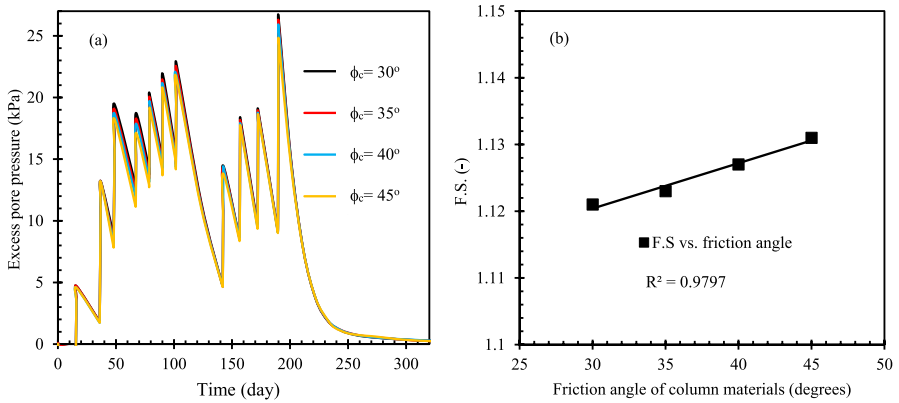


**Fig. 15** Influence of friction angle of column materials on **a** excess pore pressure in the middle of clay; **b** factor of safety at the end of construction

diameter and their spacing are kept constant equal to 80 cm and 2 m, respectively. The stiffness of the basal geogrid ranges within the values presented in Table 3 as recommended by well-known literature (EBGEO, 2010).

Figure 17a represents the variations of settlement vs. time at the end of wall construction for different values of basal geogrid stiffness. As illustrated, increasing the basal geogrid stiffness reduces the magnitude of the maximum settlement under the wall toe. The stiffer basal geogrid also causes the settlement-time curve to exhibit a gentle trend, which may result in a boosted consolidation time as stiffer geogrid redistributes the vertical stress under the RSW.

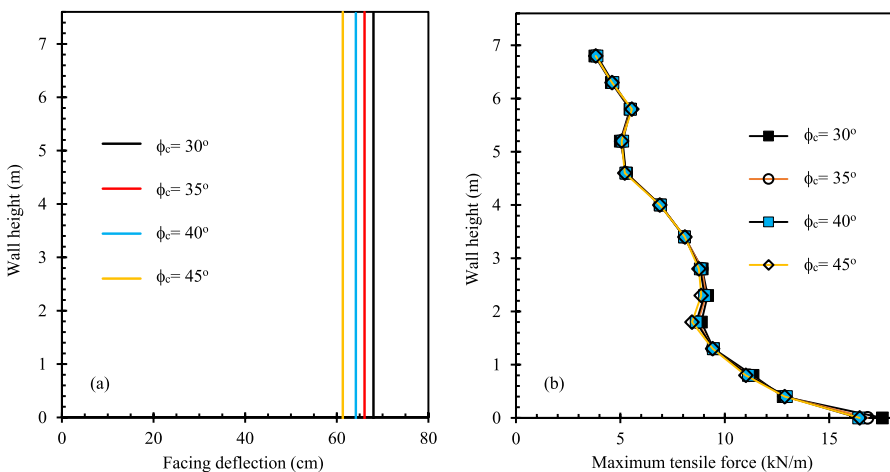


**Fig. 16** Influence of friction angle of column materials on the performance of the wall: **a** facing deflection; **b** geogrid maximum tensile force

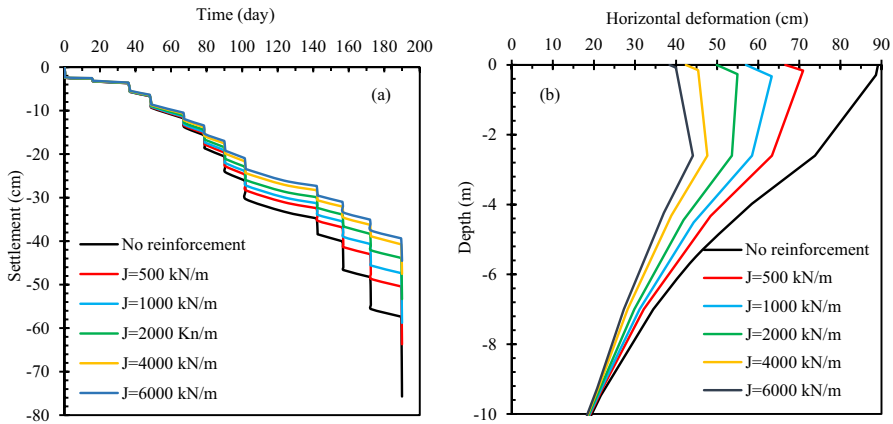


**Fig. 17** Influence of basal geogrid reinforcement on total deformations of the wall: **a** settlement vs. time; **b** profile of soil horizontal deformation ( $S = 2$  m,  $d_c = 80$  cm,  $c_s = 15$  kPa,  $\phi_c = 38^\circ$ )

The subsoil horizontal deformation shown in Fig. 17b indicates that using stiffer basal geogrid combined with granular columns decreases noticeably the maximum magnitude of horizontal displacements of the underlying soil. For instance, using a geogrid with an axial stiffness of 6000 kN/m results in the maximum value of soil horizontal displacement decreasing to half compared to when there is no reinforcement. Results of numerical analyses also indicate that there is no significant improvement in horizontal deformation under the wall toe for the basal geogrid stiffness values greater than 4000 kN/m.

Figure 18a shows the effect of basal geogrid stiffness on excess pore pressure development and dissipation in the middle of the first clay layer. The fill arching (i.e., vertical stress concentration) over granular columns could be further improved by the presence of the basal reinforcement and this phenomenon

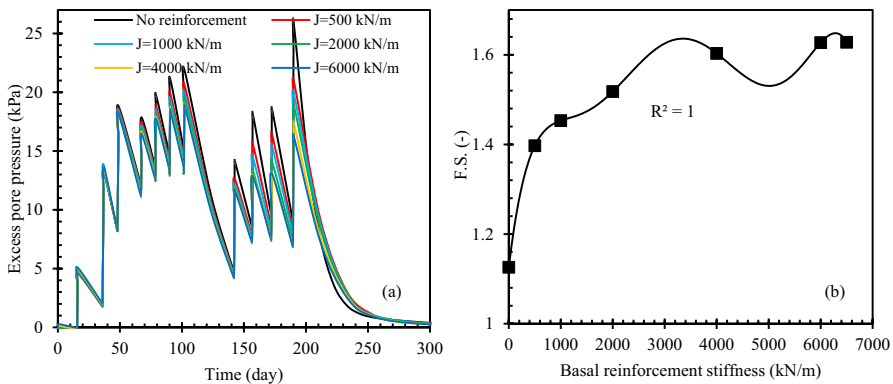


**Fig. 18** Influence of basal reinforcement on **a** excess pore pressure in the middle of clay; **b** factor of safety at the end of construction

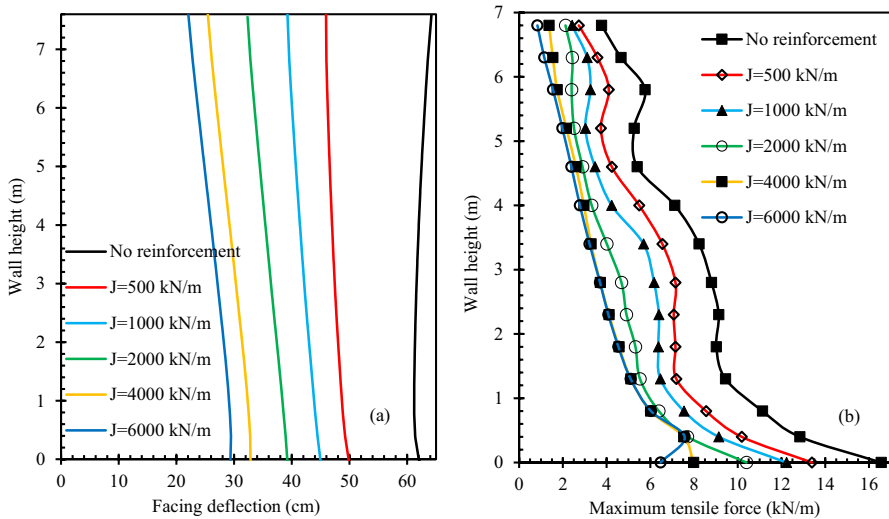


**Fig. 19** Influence of basal reinforcement on the performance of the wall: **a** facing deflection; **b** geogrid maximum tensile force

is noticeably progressed as a stiffer basal geogrid is used. For example, placing a basal geogrid with axial stiffness of 6000 kN/m causes the peak excess pore pressure at the end of wall construction to reduce to half compared to when there is no basal reinforcement. The basal geogrid, however, would not change the drainage capability of the granular columns; therefore, the dissipation time is almost unchanged. Variations of the factor of safety at the end of wall construction shown in Fig. 18b indicate that an increase in basal geogrid stiffness augments the magnitude of F.S. which is indirect evidence of progressing stress concentration over granular columns as a stiffer basal geogrid is used. For instance, using a basal geogrid with axial stiffness of 4000 kN/m increases F.S. value about 45% compared to when there is no basal geogrid thus enhancing wall stability over compressible soil layer.

A parametric study is further extended on the influence of the basal geogrid axial stiffness on RSW short-time performance. As shown in Fig. 19a, numerical results indicate that stiffer basal geogrid significantly impedes extensive facing deflection. It is seen that using basal geogrid with axial stiffness of 6000 kN/m decreases the facing deflection to half compared to when there is no basal reinforcement. This behavior is similarly observed for the maximum tensile force mobilized along with the wall reinforcement layers. As shown in Fig. 19b, increasing basal geogrid axial stiffness from 500 kN/m to 6000 kN/m was shown to reduce the tensile force in the lowermost reinforcement layer from 16 kN/m to about 6.5 kN/m.

## 5 Conclusions

Finite element analyses were conducted aiming to study the effectiveness of granular columns on the short-term behavior of RSW built on a soft foundation. To this end, equivalent column wall methodology was used to simulate granular columns in the plane strain condition and then the effect of granular columns and soft soil properties was investigated. The main conclusions of this study are listed below:

- Results of the parametric study showed that larger column diameter significantly enhanced wall performance on soft soil by decreasing wall total deformations, accelerating consolidation, improving wall short time stability, and decreasing facing deflections, as well as reducing mobilized tensile force in backfill reinforcements.
- It was found that the wall performance was greatly improved by reducing columns' center-to-center spacing as settlement and horizontal deformation under the wall toe were noticeably lowered. In addition, excess pore pressure was considerably reduced and consolidation time was accelerated as columns' spacing decreased.
- Similarly, wall stability during construction was improved as columns were installed in closer spacing. It can be concluded that column geometrical properties including both diameter and spacing play a significant role in enhancing wall performance on the soft foundation. The friction angle of column materials, however, had a negligible effect on wall performance.
- Generally, stiffer geogrid reinforcement placed at the base of the wall was found to remarkably improve the general performance of the wall over soft soil. Nevertheless, using a basal geogrid with a stiffness value over 4000 kN/m did not result in a considerable improvement in the present wall performance.

**Acronyms**  $\gamma_{\text{unsat}}$ : Unsaturated unit weight of soil ( $\text{kN/m}^3$ );  $\gamma_{\text{sat}}$ : Saturated unit weight of soil ( $\text{kN/m}^3$ );  $\gamma_c$ : Unit weight of column materials ( $\text{kN/m}^3$ );  $k_{\text{hp}}$ : Equivalent horizontal permeability in plane strain condition (m/day);  $k_{\text{hv}}$ : Equivalent vertical permeability in plane strain condition (m/day);  $E_{\text{ref}}^{50}$ : Secant elastic modulus of soil at confining pressure of 100 kPa (MPa);  $E_{\text{ogd}}^{\text{ref}}$ : Oedometric elastic modulus of soil (MPa);  $E_{\text{ur}}^{50}$ : Elastic modulus of soil for unloading and reloading (MPa);  $E_c$ : Elastic modulus of individual granular column (MPa);  $E_w$ : Elastic modulus of column-wall (MPa);  $m$ : Power for stress-level dependency of stiffness (-);  $\nu$ : Poisson's ratio (-);  $a_r$ : Area replacement ratio (-);  $c_s$ : Cohesion of soft soil (kPa);  $c_w$ : Cohesion of column-wall (kPa);  $\phi_c$ : Friction angle of individual granular column ( $^\circ$ );  $\phi_w$ : Friction angle of column-wall ( $^\circ$ );  $\phi_s$ : Friction angle of soft soil ( $^\circ$ );  $d_c$ : Column diameter (cm);  $S$ : Columns' center-to-center spacing (m);  $J$ : Reinforcement stiffness (kN/m)

**Author Contribution** It is declared that all the authors whose names are presented in the paper have successfully contributed to this paper.

**Funding** No funding is applicable to this paper.

**Data Availability** All the data, codes, and results presented in the paper are available upon request from the corresponding author.

## Declarations

**Competing Interests** The authors declare no competing interests.

**Ethics Approval and Consent to Participate** Not applicable.

## References

- Abusharar, S.M., Han, J.: Two-dimensional deep-seated slope stability analysis of embankments over stone column-improved soft clay. *Eng. Geol.* **120**(1–4), 103–110 (2011)
- Aghili, E., Hosseinpour, I., Chenari, R.J., Ahmadi, H.: Behavior of granular column-improved clay under cyclic shear loading. *Transportation Geotechnics* **31**, 100654 (2021)
- Alkhorshid, N.R., Araujo, G.L.S., Palmeira, E.M.: Consolidation of soft clay foundation improved by geosynthetic-reinforced granular columns: Numerical evaluation. *Rock Mechanics and Geotechnical Engineering* (2021). <https://doi.org/10.1016/j.jrmge.2021.03.004>
- Almeida, M.S.S., Marques, M.E.S.: Design and performance of embankments on very soft soils. Taylor & Francis CRC Press, London (2013)
- Almeida, M.S.S., Riccio, M., Hosseinpour, I., Alexiew, D.: Geosynthetic encased columns for soft soil improvement. Taylor & Francis CRC Press, London (2018)
- Ambily, A.P., Gandhi, S.R.: Behavior of stone columns based on experimental and FEM analysis. *Journal of Geotechnical and Geoenvironmental Engineering* **133**(4), 405–415 (2007)
- Bahadori, H., Farzalizadeh, R., Barghi, A., Hasheminezhad, A.: A comparative study between gravel and rubber drainage columns for mitigation of liquefaction hazards. *Rock Mechanics and Geotechnical Engineering* **10**(5), 924–934 (2018)
- Barron, R.A.: Consolidation of fine grained soils by drain wells. *Transactions of ASCE* **113**, 718–724 (1948)
- Bathurst, R.J., Naftchali, F.M.: Geosynthetic reinforcement stiffness for analytical and numerical modeling of reinforced soil structures. *Geotext. Geomembr.* **49**(4), 921–940 (2021)
- Briaud, J.L.: *Geotechnical Engineering: Unsaturated and Saturated Soils*. John Wiley & Sons, New Jersey (2013)
- Brinkgreve, R.B.J., Vermeer, P.A.: PLAXIS: *Finite element code for soil and rock analyses*. CRC Press, Balkema, Leiden, Netherlands Version **8**, 6 (2002)
- Chenari, R.J., Khonachah, R.E., Hosseinpour, I., Khajeh, A.: An experimental study for the cyclic interface properties of the EPS–sand mixtures reinforced with geogrid. *International Journal of Civil Engineering* **18**(2), 151–159 (2020)
- Chen, J.F., Liu, J., Shi, M., Xue, J.F.: Stability analyses of a reinforced soil wall on soft soils using strength reduction method. *Eng. Geol.* **177**, 83–92 (2014)
- Damians, I.P., Bathurst, R.J., Josa, A., Lloret, A.: Numerical study of the influence of foundation compressibility and reinforcement stiffness on the behavior of reinforced soil walls. *Int. J. Geotech. Eng.* **8**(3), 247–259 (2014)
- EBGEO: Recommendations for design and analysis of earth structures using geosynthetic reinforcements. German Geotechnical Society (DGGT), Berlin (2010)
- Ehrlich, M., Mirmoradi, S.H.: Evaluation of the effects of facing stiffness and toe resistance on the behavior of GRS walls. *Geotext. Geomembr.* **40**, 28–36 (2013)
- Ezzain, F., Bathurst, R.J.: Influence of foundation compressibility on reinforced soil retaining wall behavior, pp. 113–120. *GéoEdmonton' 08*, Edmonton, Canada (2008)
- Fagundes, D.F., Almeida, M.S.S., Thorel, L., Blanc, M.: Load transfer mechanism and deformation of reinforced piled embankments. *Geotext. Geomembr.* **45**(2), 1–10 (2017)
- Ghorbani, A., Hosseinpour, I., Shormage, M.: Deformation and stability analysis of embankment over stone column-strengthened soft ground. *KSCE J. Civ. Eng.* **25**(2), 404–416 (2021)
- Girout, R., Blanc, M., Dias, D., Thorel, L.: Numerical analysis of a geosynthetic-reinforced piled load transfer platform-Validation on centrifuge test. *Geotext. Geomembr.* **42**(5), 525–539 (2014)
- Han, J.: Recent research and development of ground column technologies. *Proceedings of the Institution of Civil Engineers-Ground Improvement* **168**(4), 246–264 (2015)
- Han, J., and Ye, S.L. (2001). Simplified method for consolidation rate of stone column reinforced foundation. *Journal of Geotechnical and Geoenvironmental Engineering*, 127(7), [https://doi.org/10.1061/\(ASCE\)1090-0241\(2001\)127:7\(597\)](https://doi.org/10.1061/(ASCE)1090-0241(2001)127:7(597)).

- Hatami, K., Bathurst, R.J.: Development and verification of a numerical model for the analysis of geosynthetic-reinforced soil segmental walls under working stress conditions. *Can. Geotech. J.* **42**(4), 1066–1085 (2005)
- Hosseinpour, I., Almeida, M.S.S., Riccio, M.: Full-scale load test and finite-element analysis of soft ground improved by geotextile-encased granular columns. *Geosynth. Int.* **22**(6), 428–438 (2015)
- Hosseinpour, I., Almieda, M.S.S., Riccio, M.: Verification of a plane strain model for the analysis of encased granular columns. *Journal of GeoEngineering* **12**(4), 97–105 (2017)
- Hosseinpour, I., Ghorbani, A., Zarei, J., Mohapatra, S.R.: Experimental study on the behavior of granular column-treated soft clay under shear loading. *Geomechanics and Geoengineering* (2022). <https://doi.org/10.1080/17486025.2021.2015977>
- Hosseinpour, I., Riccio, M., Almeida, M.S.S.: Field-measured Poisson's ratio of geotextile-encased granular column. *Proceedings of the Institution of Civil Engineers -Ground Improvement* **174**(2), 63–69 (2021)
- Hosseinpour, I., Riccio, M., Almeida, M.S.S.: Numerical evaluation of a granular column reinforced by geosynthetics using encasement and laminated disks. *Geotext. Geomembr.* **42**(4), 363–373 (2014)
- Hosseinpour, I., Soriano, C., Almedia, M.S.S.: A comparative study for the performance of encased granular columns. *Rock Mechanics and Geotechnical Engineering* **11**(2), 379–388 (2019)
- Lima, B., Almeida, M.S.S., Hosseinpour, I.: Field measured and simulated performance of a stone columns-strengthened soft clay deposit. *Int. J. Geotech. Eng.* (2019). <https://doi.org/10.1080/19386362.2019.1653506>
- Mirmoradi, S.H., Ehrlich, M.: Numerical evaluation of the behavior of GRS walls with segmental block facing under working stress conditions. *Geotechnical and Geoenvironmental Engineering* **141**(3), 04014109 (2015)
- Mirmoradi, S.H., Ehrlich, M.: Evaluation of the effect of toe restraint on GRS walls. *Transportation Geotechnics* **8**, 35–44 (2016)
- Mirmoradi, S.H., Ehrlich, M.: Effects of facing, reinforcement stiffness, toe resistance, and height on reinforced walls. *Geotext. Geomembr.* **45**(1), 67–76 (2017)
- Mirmoradi, S.H., Ehrlich, M., Magalhães, L.F.O.: Numerical evaluation of the effect of foundation on the behaviour of reinforced soil walls. *Geotext. Geomembr.* **49**(3), 619–628 (2021)
- Palmeria, E.M., and Monte, L.M. (1997). The behaviour of model reinforced walls on soft soils. *Geosynthetics '97*, Long Beach California, USA, 11–13 March 1997. Industrial Fabrics Association International, pp. 73–84.
- Rowe, R.K., and Ho, S.K. (1993). Keynote lecture: a review of the behavior of reinforced soil walls. *Earth Reinforcement Practice*. In: In: Ochiai, H., Hayashi, S., Otani, J. (Eds.), *Proc. Int. Symposium on Earth Reinforcement Practice*, vol. 2. Kyushu University, Fukuoka, Japan, pp. 801–830 Balkema, Rotterdam, Netherlands.
- Rowe, K., Skinner, G.D.: Numerical analysis of geosynthetic reinforced retaining wall constructed on a layered soil foundation. *Geotext. Geomembr.* **19**(7), 387–412 (2001)
- Sexton, B.G., McCabe, B.A., Karstunen, M., Sivasithamparam, N.: Stone column settlement performance in structured anisotropic clays: the influence of creep. *Rock Mechanics and Geotechnical Engineering* **8**(5), 672–688 (2016)
- Srikar, G., and Mittal, S. (2020). Seismic analysis of retaining wall subjected to surcharge: a modified pseudo-dynamic approach. *International Journal of Geomechanics*, 20(9), [https://doi.org/10.1061/\(ASCE\)GM.1943-5622.0001780](https://doi.org/10.1061/(ASCE)GM.1943-5622.0001780).
- Schmertmann, G.R., Chew, S.H., and Mitchell, J.K. (1989). *Finite element modelling of reinforced soil wall behavior*. Department of Civil Engineering, University of California, Berkeley. Geotechnical Engineering Report No. UCB/GT/89–01.
- Tandel, Y.K., Solanki, C.H., Desai, A.K.: Reinforced stone column: remedial of ordinary stone column. *International Journal of Advances in Engineering & Technology* **3**(2), 340–348 (2012)
- Yoo, C.: Settlement behavior of embankment on geosynthetic-encased stone column installed soft ground-A numerical investigation. *Geotext. Geomembr.* **43**(6), 484–492 (2015)
- Zhang, Z., Han, J., Ye, G.: Numerical investigation on factors for deep-seated slope stability of stone column-supported embankments over soft clay. *Eng. Geol.* **168**, 104–113 (2014)
- Zheng, G., Yu, X., Zhou, H., Wang, S., Zhao, J., He, X., Yang, X.: Stability analysis of stone column-supported and geosynthetic-reinforced embankments on soft ground. *Geotext. Geomembr.* **48**(3), 349–356 (2019)



## Authors and Affiliations

**Amir Hossein Mirrashed<sup>1</sup> · Iman Hosseinpour<sup>1</sup> · Seyed Hamed Mirmoradi<sup>2</sup> · Hadi Ahmadi<sup>3</sup>**

Amir Hossein Mirrashed  
amirmirrashed15@gmail.com

Seyed Hamed Mirmoradi  
shm@ufrj.br

Hadi Ahmadi  
hadiahmadi@guilan.ac.ir

- <sup>1</sup> Civil Engineering Department, Faculty of Engineering, University of Guilan, Persian Gulf Highway, PB: 41996-13776, Rasht, Guilan, Iran
- <sup>2</sup> Civil Engineering Department (PEC), Graduate School in Research and Engineering (COPPE), Federal University of Rio de Janeiro (UFRJ), Ilha de Fundao, RJ, CEP: 21945-970, Brazil
- <sup>3</sup> Civil Engineering Department, Faculty of Technology and Engineering (Eastern Guilan), P.B: 44918-98566, Rudsar, Guilan, Iran